A Crystal Structure Determination of PbC_2O_4 from Synchrotron X-Ray and Neutron Powder Diffraction Data

A. Nørlund Christensen,[a] D. E. Cox[b] and M. S. Lehmann[c]

[a]Department of Inorganic Chemistry, Aarhus University, DK-8000 Aarhus C, Denmark, [b]Brookhaven National Laboratory, NSLS, Upton, New York 11973, U.S.A. and [c]Institut Max von Laue – Paul Langevin, 156 x, F-38042 Grenoble Cedex, France

Christensen, A. N., Cox, D. E. and Lehmann, M. S., 1989. A Crystal Structure Determination of PbC_2O_4 from Synchrotron X-Ray and Neutron Powder Diffraction Data. – Acta Chem. Scand. 43: 19–25.

The crystal structure of lead oxalate, PbC_2O_4, was solved *ab initio* from synchrotron X-ray and neutron diffraction powder patterns. The unit cell was obtained by auto-indexing of Guinier film data, the basic features of the structure were solved using direct methods and integrated intensities obtained from high resolution synchrotron X-ray data, and the structure was refined by Rietveld analysis of these and high resolution neutron data. Although there were serious discrepancies in the overall profile fit of the X-ray data because of pronounced anisotropic peak broadening, the two sets of positional coordinates were in good agreement.

The unit cell is triclinic, space group $P\bar{1}$ (No. 2) with lattice parameters from the synchrotron refinement: $a = 555.70(1)$, $b = 697.72(1)$, $c = 557.26(1)$ pm, $\alpha = 109.554(1)$, $\beta = 113.610(1)$, $\gamma = 88.802(1)°$, $Z = 2$. The structure has two crystallographically independent oxalate ions stacked in layers alternating with layers of lead ions in the [001] direction. The oxalate ions form channels along the b axis in which the lead ions are situated in highly asymmetric coordination with seven oxygen atoms.

Individual peak fits of the synchrotron data revealed all of the reflections to be broadened appreciably by comparison with the instrumental resolution. Those with scattering vectors close to the [001] axis showed an additional systematic broadening consistent with stacking faults in this direction.

The continuing development of high-resolution neutron and X-ray powder techniques is stimulating widespread interest in the solution of complex crystal structures *ab initio* from powder diffraction data. The advantage of using high-resolution diffractometers is that even powder patterns of rather complicated nature with overlapping reflections may be deconvoluted into individual intensities that can be used in solving a crystal structure employing standard single-crystal techniques. When a model for the structure is found, refinement of the model is made using the profile analysis least-squares procedure proposed by Rietveld.[1] Some of the general considerations involved in solving structures *ab initio* from powder data have been discussed in a recent paper,[2] and examples of the use of these techniques are provided by the structure determinations of $Al_2Y_4O_9$,[3] I_2O_4,[3] α-$CrPO_4$,[4] $(NH_4)_4[(MoO_2)_4O_3](C_4H_3O_5)_2$,[5] $FeAsO_4$[6] and $ZrNaH(PO_4)_2$.[7]

The present work reports an *ab initio* determination of the triclinic structure of lead oxalate, PbC_2O_4, from powder data by combining information from X-ray and neutron diffraction patterns. The unit cell was obtained by automatic indexing of a Guinier pattern, the basic structural features were established by direct methods of analysis from integrated intensities obtained from a well-resolved synchrotron X-ray pattern, and the structure was refined by Rietveld analysis of the synchrotron and the high-resolution neutron diffraction data.

Experimental

Sample preparation. The white crystalline powder of PbC_2O_4 was prepared from $Pb(NO_3)_2$ (B.D.H. analytical grade) and $(NH_4)_2C_2O_4 \cdot H_2O$ (Merck *p.a.*). A solution of 6.0 g of ammonium oxalate in 100 ml of water was added dropwise to a solution of 14.0 g of lead nitrate in 100 ml of water. The precipitated lead oxalate was thoroughly washed with water and dried at 120° for 24 h.

X-Ray diffraction. Guinier photographs of PbC_2O_4 were taken using Si ($a = 543.050$ pm) as an internal standard and Cu$K\alpha_1$ radiation ($\lambda = 154.0598$ pm). The positions and intensities of the diffraction lines were measured on a double-beam photometer, and the powder pattern was then indexed using the program FZON.[8] The values obtained were $a = 556.07(3)$, $b = 698.26(3)$, $c = 557.71(3)$ pm, $\alpha = 109.551(3)$, $\beta = 113.620(3)$, $\gamma = 88.814(4)°$, and the space group $P\bar{1}$ was assumed. This choice of unit cell is different from that reported previously.[9] Assuming $Z = 2$, the calculated density is 5.30 g cm^{-3}, which may be compared to the reported value for the density of 5.28 g cm^{-3}.[10]

The powder diffraction pattern was also recorded with synchrotron X-ray radiation using the diffractometer on the X13 A beam line at the Brookhaven National Synchrotron Light Source (NSLS). The wavelength used was 131.5 pm, and the sample was a flat plate of PbC_2O_4. A detailed

description of the diffractometer is reported elsewhere.[11] The powder pattern was measured in the 2θ range 10–70°, at step intervals of 0.01°, and the sample was oscillated through a few degrees during data collection to ensure proper particle randomization.

Neutron diffraction. The powder neutron diffraction pattern was recorded on the D2B diffractometer at the Institut Laue-Langevin, Grenoble, using a wavelength of 159.50 pm.[12] This instrument has an array of 64 detectors spaced 2.5° apart. Thus by making a total scan of 2.5°, a full pattern is obtained. The step length used in this measurement was 0.025°. In the present case the highest detector angle was 150°, thus giving a 2θ range of 13–150°, the data below 13° being obscured by the beam stop.

Structure determination

Assuming the centrosymmetric space group $P\bar{1}$, the unit cell contains two Pb^{2+} and two $C_2O_4^{2-}$ ions. Structure factors were calculated from the Guinier photographs and an attempt was made to solve the structure with these data by direct methods using the MULTAN program.[13] In this calculation 46 observed structure factors were used together with 25 which were not observed. This calculation did not give a clear centrosymmetric solution, but rather one in which the vector between the two highest peaks in the electron density map was (0.5, 0.5, 0.2). If this is interpreted as a Pb-Pb vector, the coordinates of the lead ion in $P\bar{1}$ would be approximately (0.25, 0.25, 0.10). A check of the visually estimated intensities of the first few lines of the Guinier photograph using only scattering contributions from the lead ions indicated that the heavy-atom position was close to that given above.

The synchrotron radiation diffraction pattern had rather better resolution of the diffraction lines than the Guinier photograph, and the measured intensities also compared well with those calculated with the program LAZY PULVERIX[14] using again only the contribution from lead. These digital data were therefore used in the following calculations. With the program ALLHKL,[15] 218 reflections with $F > \sigma(F)$ and 4 reflections with $F < \sigma(F)$ were extracted. This new set of structure factors was used to determine the structure by direct methods (MULTAN).[13] Again, the calculations did not give a clear centrosymmetric solution but a vector between the two highest peaks of (0.5073, 0.5071, 0.1763). In the space group $P\bar{1}$ this corresponds to a lead atom position of (0.2537, 0.2535, 0.0882). Using the 218 structure amplitudes in a series of structure factor and Fourier map calculations, the positions of six oxygen/carbon atoms were found. This set of coordinates was then used in a preliminary Rietveld refinement of the synchrotron radiation diffraction pattern with the program EDINP.[16] The atomic scattering factors used in the calculations were the neutral atom values reported by Cromer and Mann.[17]

At this stage, the precision of the oxygen/carbon positions of the model was low, and it was difficult to locate the oxalate ion among the six atoms. This is not surprising since the average scattering contribution per atom to the intensity for X-rays is: Pb: 95 %, C: 0.5 %, O: 1.0 %. In the neutron diffraction case, the average scattering contribution per atom would be: Pb: 29.5 %, C: 14.0 %, O: 10.6 %, and the neutron data are thus much better for the determination of the positions of the atoms in the $C_2O_4^{2-}$ ion. Consequently, the neutron powder diffraction pattern was used in a Rietveld refinement of the structure of PbC_2O_4. The scattering lengths used were: Pb: 0.940, C: 0.665, O: 0.581 (all in 10^{-12} cm units),[18] and the program used was the Hewat version[19] of the Rietveld program.[1] Starting parameters were the coordinates from the preliminary refinement of the X-ray synchrotron data. A total of 40 parameters were refined, viz. the positional coordinates and individual isotropic temperature factors for seven atoms, six lattice parameters, three half-width parameters, an asymmetry parameter, a zero-point correction and a scale factor. Background values were obtained by interpolation, and contributions were taken from each peak over a range of

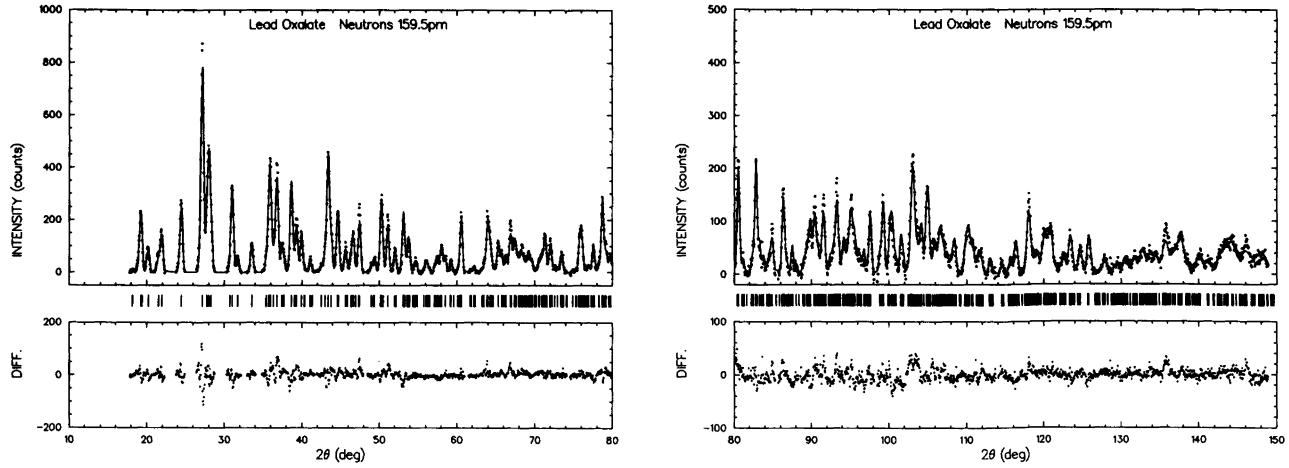

Fig. 1. Profile fit of neutron powder diffraction data. Differences are given in the lower part of the figures. Allowed reflections are indicated by short vertical markers.

Table 1. Coordinates and temperature factors for X-ray and neutron data. The X-ray profiles were described with a pseudo Voigt function with a Gaussian half-width given as $(U\tan^2\theta + V\tan\theta + W)^{1/2}$ and a Lorentzian half-width of $X\tan\theta + Y/\cos\theta$. For the case of neutrons only a Gaussian was used. The R factors and the goodness of fit index S_p^2 are defined as follows: $R_I = \Sigma\,|I_{obs} - I_{calc}|\,/\,\Sigma\,I_{obs}$, where the I values are approximate integrated intensities derived from the powder profiles using the procedure described by Rietveld,[a] $R_{wp} = [\Sigma\,(y_{obs} - y_{calc})^2\,W/\Sigma\,y_{obs}^2\,W]^{1/2}$, where the y values are the profile intensities with the background y_b subtracted, and $W = 1/(y_{obs} + y_b)$, $R_E = [(N-M)/\Sigma\,y_{obs}^2\,W]^{1/2}$ and $\sqrt{S_p^2} = [\Sigma\,(y_{obs} - y_{calc})^2\,W/(N-M)]^{1/2}$, where N and M are the number of profile points and variable parameters, respectively.

	X-Ray				Neutron			
	x	*y*	*z*	*B*/Å²	*x*	*y*	*z*	*B*/Å²
Pb	0.2641(3)	0.2572(2)	0.0940(3)	0.34(3)	0.2621(6)	0.2571(6)	0.0933(6)	1.27(6)
C(1)	0.639(5)	0.039(4)	0.542(5)	−1.5(6)	0.6446(9)	0.0466(7)	0.5459(10)	1.50(9)
C(2)	0.133(5)	0.492(4)	0.623(5)	−0.4(6)	0.1293(9)	0.4992(7)	0.6294(10)	1.45(9)
O(1)	0.694(3)	0.155(3)	0.426(3)	−0.3(4)	0.6904(11)	0.1397(9)	0.4121(12)	2.37(12)
O(2)	0.804(3)	0.020(2)	0.735(3)	−0.8(4)	0.8194(12)	0.0142(9)	0.7559(12)	2.29(11)
O(3)	0.299(4)	0.423(3)	0.588(4)	1.2(6)	0.3091(10)	0.4195(8)	0.5770(11)	1.48(10)
O(4)	0.131(3)	0.582(3)	0.860(4)	0.6(5)	0.1245(12)	0.5782(8)	0.8582(12)	2.03(12)
R_I	10.0				10.1			
R_{wp}	21.3				17.9			
R_E	5.7				16.8			
S_p^2	3.7				1.1			
a/pm	555.703(9)				556.25(2)			
b/pm	697.718(11)				698.44(3)			
c/pm	557.257(9)				557.84(2)			
α/°	109.5535(10)				109.554(3)			
β/°	113.6104(9)				113.616(3)			
γ/°	88.8022(11)				88.813(3)			
$U/°^2$	0.0512(38)				0.1189(40)			
$V/°^2$	−0.0270(22)				−0.1932(51)			
$W/°^2$	0.0062(3)				0.2140(30)			
X/°	0.071(6)							
Y/°	0.015(1)							

[a]Ref. 1.

1.5 FWHM on each side of the peak maximum. A total of 700 reflections were included in the refinement. The results are listed in Table 1, and the profile fit and difference plot are shown in Fig. 1.

Thus, with the structure solved and the carbon and oxygen atoms in the oxalate ions unambiguously located, further Rietveld refinement was performed using the synchrotron X-ray data and a modified version of the Hewat program. In this, the peak shapes are assumed to be the convolution of Gaussian and Lorentzian functions, with respective FWHM's Γ_G and Γ_L taken as

$$\Gamma_G = (U\tan^2\theta + V\tan\theta + W)^{1/2}$$

$$\Gamma_L = X\tan\theta + Y/\cos\theta$$

where U, V, W, X and Y are refinable parameters which take into account instrumental resolution and sample broadening effects. In this case, contributions from each peak were taken over a range of 5 FWHM on either side of the peak because of the much longer tails. A total of 250 reflections were included in the refinement. The results are listed in Table 1, and the profile fit and difference plot are illustrated in Fig. 2.

Comparison of the R factors obtained from the two refinements reveals that although the integrated intensity residuals are essentially identical, the profile goodness-of-fit index ($R_{wp}/R_E = \sqrt{S_p^2}$) for the X-ray refinement is 3.7, which is high compared to the neutron value of 1.1. This is reflected in the profile fit in Fig. 2, where a number of pronounced discrepancies are quite evident. The main reason for this is the highly anisotropic nature of the peak widths, as can be seen from some individual peak fits displayed in Fig. 3 and listed in Table 2. In these fits, individual values of Γ_G and Γ_L were refined for each peak in addition to intensity peak position and background, and the goodness-of-fit indices were generally in the range 1.0–1.3, which shows that the peak shapes are described well by the function. The results in Table 2 show that some closely adjacent peaks have FWHM's differing by factors of two to three.

However, despite the discrepancies in the overall profile fit, the refinement converged to atomic positions in quite respectable agreement with the neutron ones, the mean deviation between the two sets of coordinates being only 2.2 times the pooled standard deviation from the Rietveld refinements. This surprisingly good agreement can be attributed to negligible correlations between atomic coordinates and the half-width parameters. Whereas correlation coefficients from the full-matrix least-squares refinement

Table 2. Selected list of full width at half maximum Γ determined from the synchrotron X-ray data using a special version of ALLHKL.[a] Γ_{obs} are the observed values for PbC_2O_4, Γ_{ref} the instrumental values determined using a Si powder and $\Delta\Gamma$ is the difference. In addition $\Delta\Gamma / \tan\theta$ and $\Delta\Gamma \cos\theta$ are listed. *V* is the angle (in degrees) between *h k l* reflections and selected *h' k' l'* directions. The data are divided into groups of *h k l*'s for which $V < 25°$ for a given *h' k' l'*. Mean values of $\Delta\Gamma / \tan\theta$ and $\Delta\Gamma \cos\theta$ are given for each group with the sampling standard deviation in parentheses. Pronounced $\tan\theta$-like broadening is seen for the 001 group of reflections.

h	*k*	*l*	2θ	Γ_{obs}	Γ_{ref}	ΔΓ	$\Delta\Gamma/\tan\theta$	$\Delta\Gamma\cos\theta$	*V*	*h'*	*k'*	*l'*
2	0	0	30.20	0.084	0.040	0.043	0.161	0.042	0			
2	−1	1	38.78	0.054	0.033	0.021	0.060	0.020	23			
2	0	1	39.98	0.042	0.032	0.010	0.028	0.010	22	1	0	0
3	1	−1	43.50	0.114	0.030	0.084	0.212	0.078	21			
3	0	0	46.00	0.094	0.029	0.065	0.152	0.060	0			
3	1	0	49.19	0.079	0.029	0.051	0.110	0.046	14			
						mean	0.12(7)	0.04(3)				
0	2	0	23.28	0.067	0.047	0.020	0.098	0.020	0			
1	−3	0	36.53	0.091	0.034	0.056	0.171	0.054	24			
1	3	0	40.34	0.054	0.032	0.022	0.060	0.021	22			
1	−3	−1	42.60	0.063	0.030	0.033	0.085	0.031	23	0	1	0
0	3	1	43.99	0.073	0.030	0.044	0.109	0.041	20			
0	4	−1	44.31	0.096	0.029	0.067	0.164	0.062	20			
0	4	0	47.60	0.077	0.029	0.048	0.110	0.044	0			
						mean	0.11(4)	0.04(2)				
0	0	1	15.84	0.088	0.054	0.034	0.242	0.033	0			
0	1	−2	29.85	0.104	0.040	0.064	0.239	0.062	22			
0	0	2	32.00	0.118	0.038	0.080	0.279	0.077	0			
0	1	2	37.99	0.123	0.033	0.090	0.260	0.085	17	0	0	1
1	0	2	41.05	0.114	0.031	0.083	0.220	0.077	20			
1	0	−3	44.43	0.155	0.029	0.126	0.309	0.117	18			
0	1	3	45.80	0.169	0.029	0.141	0.333	0.130	14			
						mean	0.27(4)	0.08(3)				
1	1	0	20.14	0.064	0.050	0.014	0.078	0.014	0			
1	2	0	29.44	0.051	0.041	0.010	0.038	0.010	17			
1	2	1	40.25	0.073	0.032	0.041	0.112	0.038	24	1	1	0
2	2	0	40.95	0.053	0.031	0.022	0.058	0.020	0			
3	1	0	49.19	0.079	0.029	0.051	0.110	0.046	21			
						mean	0.08(3)	0.03(2)				
1	−1	0	17.71	0.085	0.052	0.033	0.212	0.033	0			
2	−2	0	35.86	0.106	0.035	0.071	0.220	0.068	0			
2	−2	1	41.23	0.081	0.031	0.050	0.133	0.047	23	1	$\bar{1}$	0
3	−1	−1	43.36	0.088	0.030	0.058	0.147	0.054	25			
						mean	0.18(4)	0.05(2)				

[a]Ref. 15.

were often above 0.3 within the two classes of parameters, they did not exceed 0.05 for elements relating the two groups. A smoothly varying function for the half-width is thus apparently not so important as one might expect at first view. Obviously, the precision will be adversely affected, as the standard deviations contain a term proportional to the goodness-of-fit index, but there is reason to hope that this kind of systematic error does not bias the structural data. Moreover, the anisotropic peak-widths contain potentially useful information concerning macroscopic effects such as particle shape, strain and stacking faults which can be extracted without undue correlation with the structural parameters. The agreement between the temperature factors from the two refinements is less satisfactory, but in this case the observed correlations between half-width parameters and the temperature factors are rather high, as might be expected. It is observed that the two sets of lattice parameters are also in excellent agreement if small errors in the assumed wavelengths are taken into account with a scaling factor of 1.00102.

Description of the structure

Table 3 summarizes the most important interatomic distances and lists similar values for the oxalate ion in CaC_2O_4,[20] and for oxalic acid.[21] As expected, the C–O distances come closest to values for the ionic form of C_2O_4, being somewhere between those for single and double bonds. Likewise, both ions are planar with a maximum distance from the plane of 1.7 pm, which is less than the error in the atomic positions. The arrangement of oxygen around lead is irregular, with seven nearest neighbours;

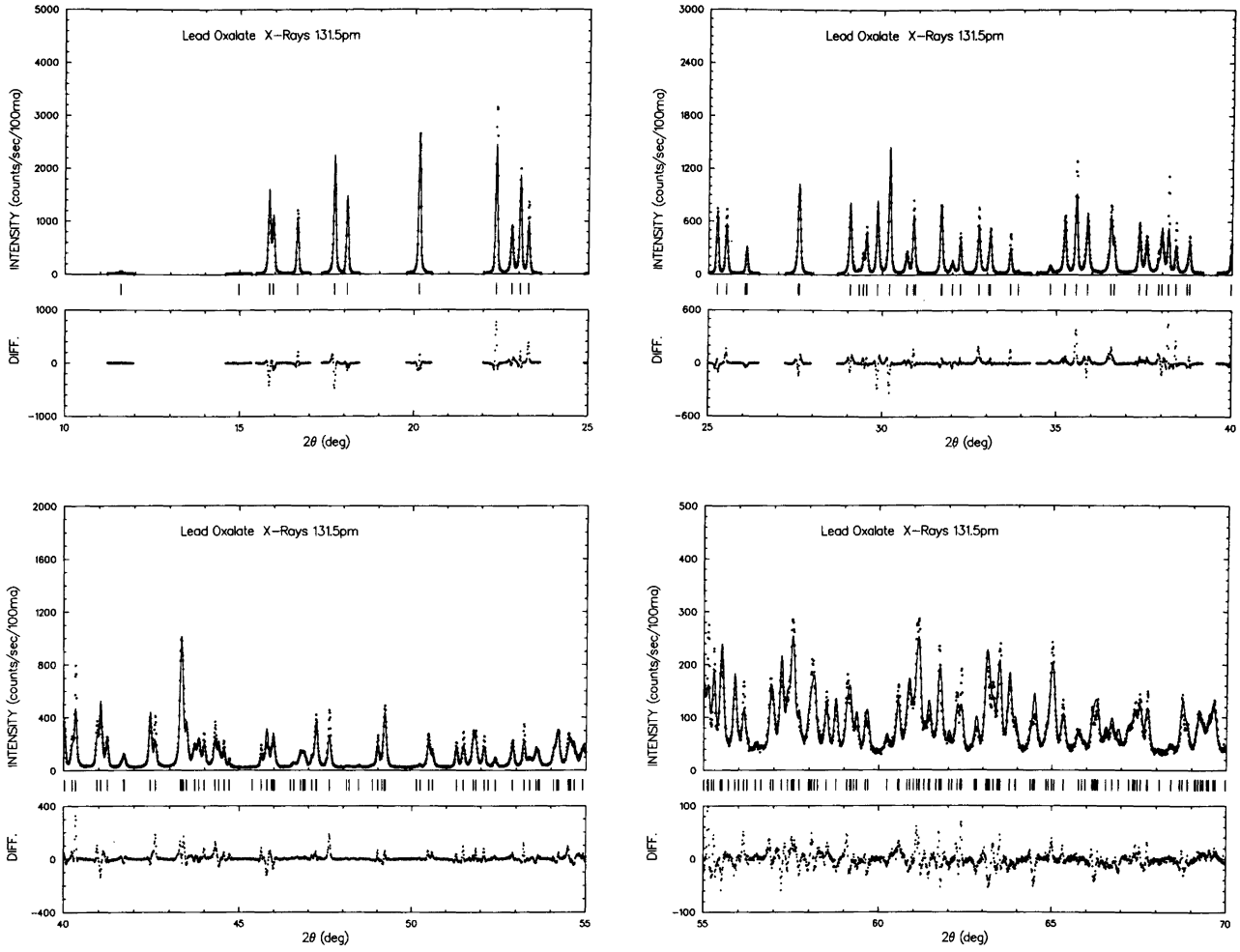

Fig. 2. Profile fit of synchrotron X-ray powder data. Differences are given in the lower part of the figures.

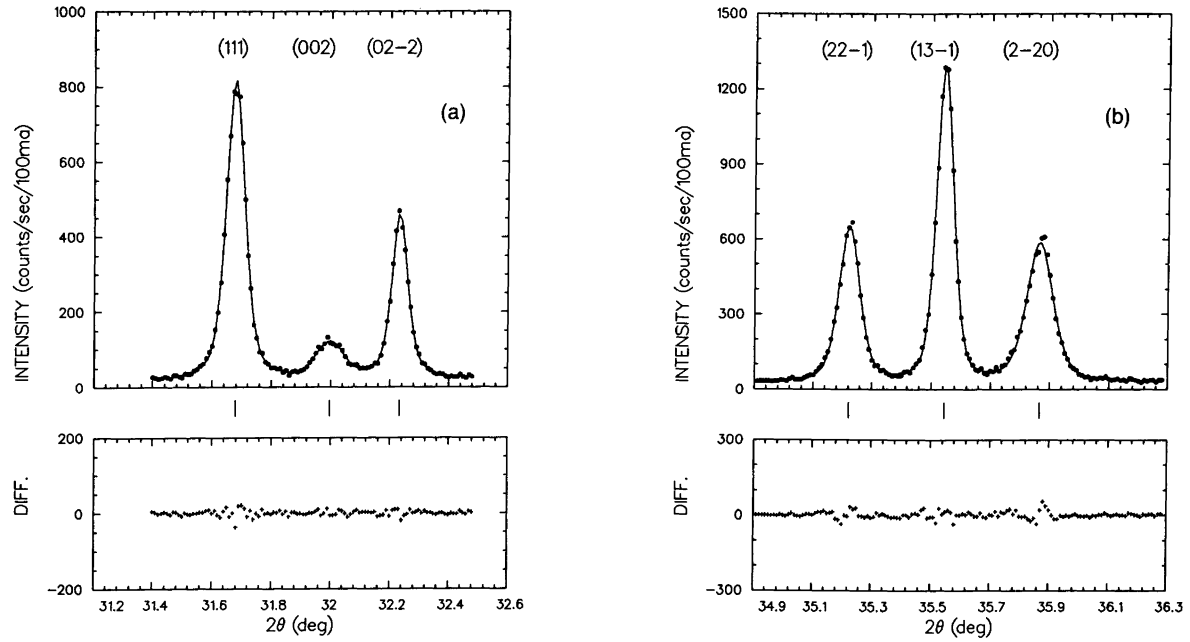

Fig. 3. Examples of individual peak fits and difference plots for selected reflections: (a) for 111, 002, $02\bar{2}$, and (b) for $22\bar{1}$, $13\bar{1}$, and $2\bar{2}0$ (synchrotron X-ray data).

Table 3. Interatomic distances in pm. For Pb the X-ray coordinates are used, and for other atoms the neutron coordinates are employed. Standard deviations in parentheses.

Pb–O2′	243.2(7)		
Pb–O3	245.6(7)		
Pb–O4′	248.5(7)		
Pb–O2	260.9(7)		
Pb–O1	264.8(7)		
Pb–O3′	284.6(7)		
Pb–O4″	290.3(8)		
		Reported distances	
		Ref. 20:	
C1–O1	123.6(9)	C–O	125.3(4)
C1–O2	127.5(9)	C–O	122.9(8)
C1–C1′	156.1(8)	C–O	124.7(8)
C2–C2′	158.1(9)	C–C	155.0(4)
C2–O3	122.4(10)	C–C	153.0(8)
C2–O4	122.0(9)		
		Ref. 21:	
		C–O	129.1(2)
		C–O	120.8(2)
		C–C	153.9(2)

this leads to a molecular packing which is quasi two-dimensional.

Corrugated layers of lead atoms are sandwiched between oxalate ions stacked into layers roughly perpendicular to the c^* axis. The oxalate ions also form fairly wide channels running along the b direction, as shown in Fig. 4. The Pb^{2+} ions are located within these channels in off-center positions, which leads to highly asymmetric coordination bearing at least a superficial resemblance to that of absorbed species in some zeolite structures.

Anisotropic peak-widths

An inspection of the refined values for the half-widths of the stronger peaks in Figs. 3(a) and (b) reveals that compared to the instrumental resolution function determined with a Si reference sample, most of the peaks are broadened to about 0.02–0.04° while a few are broadened much more, viz. to 0.05–0.1°. We have attempted an analysis of the broadening with a very simple model in which reflections are classified according to whether their scattering vectors lie within 25° of the following directions: [100], [010], [001], [110] and [1$\bar{1}$0]. The observed broadening, $\Delta\Gamma$, is taken as the difference between the observed and instrumental FWHM's (Table 2). Also tabulated are the normalized values $\Delta\Gamma\cos\theta$ and $\Delta\Gamma/\tan\theta$ which allow for the angular dependence of particle size (Scherrer) broadening and strain/stacking disorder broadening. From these results it is seen that reflections with scattering vectors close to [001] show a pronounced systematic broadening with a $\tan\theta$ dependence characteristic of microscopic strain or stacking faults. For the other directions the broadening is smaller, and no readily identifiable angular dependence is seen.

As noted above, the structure consists of alternating layers of lead and oxalate ions along the [001] axis. The main bonding force is undoubtedly the electrostatic interaction between layers, while the interactions between the

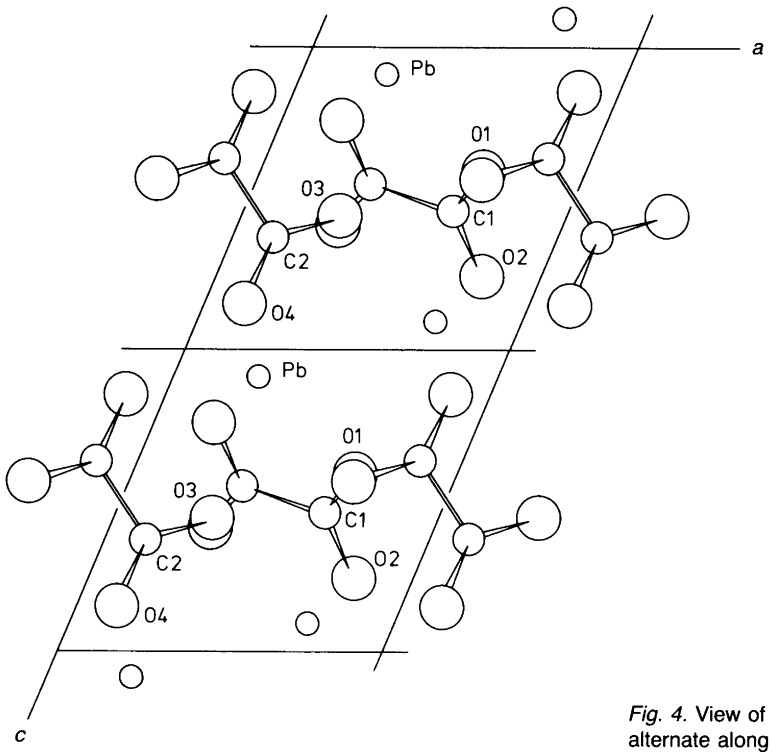

Fig. 4. View of the structure along *b*. Layers of lead and oxalate ions alternate along the c^* direction. Two unit cells are shown.

oxalate ions are of secondary importance. These ions have no overall dipole moments, and the near contact between O(1) and O(3) of 290 pm, only slightly more than twice the van der Waals contact of oxygen, does little to stabilize the oxalate layers. The crystals grow quickly by precipitation, and from the bonding forces it is thus anticipated that the main growth direction is along c^*, orthogonal to the layers. It seems quite plausible that packing irregularities in the oxalate layers could readily occur, and could lead to stacking faults along this growth direction and a corresponding broadening of this class of reflections.

Summary

When a compound with very low solubility is prepared by precipitation in an aqueous solution, crystals of a size suitable for single crystal analysis will normally not be formed, and one must then rely on *ab initio* structure determination based on high-resolution powder data. This is not necessarily a straightforward technique, as illustrated by the present study which exemplifies well the various steps in the process. Indexing of the pattern is accomplished from high precision X-ray diffraction data, and the main features of the structure are then solved from the integrated X-ray intensities, a process which is greatly facilitated by the presence of a heavy atom. The light-atom positions are confirmed using neutron diffraction data, and structure refinement using the two sets of data then allows a realistic estimate of the accuracy of the structural parameters. It is here worth noting that the X-ray data allow a determination of light-atom positions in the presence of Pb within an esd of about 2 pm, which would be considerably less but for the presence of anisotropic peak broadening.

The analysis shows that the structure consists of alternating layers of lead and oxalate ions. The crystals grow quickly during precipitation, and from this it is possible to suggest a simple mechanism to explain the principal feature of the anisotropic peak broadening. Because of the triclinic symmetry a more generalized analysis is not worthwhile, but for higher symmetry structures this kind of approach could clearly be extended. The high resolution X-ray data therefore allow not only the solution of non-trivial structural problems but also give some indication of how the crystal is organized on a semi-macroscopic level.

Acknowledgements. This investigation was supported in part by NATO, grant No. 86/0551. In addition, we thank Dr. A. W. Hewat for interest in this study. Part of the research was carried out at the National Synchrotron Light Source, Brookhaven National Laboratory, which is supported by the U.S. Department of Energy, Division of Materials Sciences and Division of Chemical Sciences. D.E.C. is grateful for support by the Division of Materials Sciences under Contract No. DE-AC02-76-CH-00016.

References

1. Rietveld, H. M. *J. Appl. Crystallogr. 2* (1969) 65.
2. Christensen, A. N., Lehmann, M. S. and Nielsen, M. *Aust. J. Phys. 38* (1985) 497.
3. Lehmann, M. S., Christensen, A. N., Fjellvåg, H., Feidenhans'l, R. and Nielsen, M. *J. Appl. Crystallogr. 20* (1987) 123.
4. Attfield, J. P., Sleight, A. W. and Cheetham, A. K. *Nature (London) 322* (1986) 620.
5. Berg, J.-E. and Werner, P.-E. *Z. Kristallogr. 145* (1977) 310.
6. Cheetham, A. K., David, W. I. F., Eddy, M. M., Jakeman, R. J. B., Johnson, M. W. and Torardi, C. C. *Nature (London) 320* (1986) 46.
7. Rudolf, P. and Clearfield, A. *Acta Crystallogr., Sect. B 41* (1985) 418.
8. Visser, J. W. *J. Appl. Crystallogr. 2* (1969) 89.
9. de Wolff, P. M. *JCPDS data card No. 14-803.* Delft University of Technology, Delft, the Netherlands.
10. Weast, R. C., Ed., *Handbook of Chemistry and Physics,* CRC Press, Cleveland 1976.
11. Cox, D. E., Hastings, J. B., Cardoso, L. P. and Finger, L. W. *Mater. Sci. Forum 9* (1986) 1.
12. Hewat, A. W. *Mat. Sci. Forum 9* (1986) 69.
13. Main, P., Lessinger, L., Woolfson, M. M., Germain, G. and Declercq, J.-P. *MULTAN*: Universities of York, England, and Louvain, Belgium 1977.
14. Yvon, K., Jeitschko, W. and Parthé, E. *J. Appl. Crystallogr. 10* (1977) 357.
15. Pawley, G. S. *J. Appl. Crystallogr. 14* (1981) 357.
16. Pawley, G. S. *J. Appl. Crystallogr. 13* (1980) 630.
17. Cromer, D. T. and Mann, J. B. *Acta Crystallogr., Sect. A 24* (1968) 321.
18. Koester, L. and Rauch, H. *Summary of Neutron Scattering Lengths,* KFA, Jülich, BRD 1981.
19. Hewat, A. W. *Harwell Report AERE, R7350,* Harwell, U.K. 1973.
20. Deganello, S. *Acta Crystallogr., Sect. B 37* (1981) 826.
21. Coppens, P. and Sabine, T. M. *Acta Crystallogr., Sect. B 25* (1969) 2442.

Received March 24, 1988.